ELSEVIER

Polymer 43 (2002) 6397–6405

polymer

www.elsevier.com/locate/polymer

Photoprotective ceramic coatings on poly(ether ether ketone)

S. Giancaterina[a], S. Ben Amor[a,1], G. Baud[a], J.L. Gardette[b,*], M. Jacquet[a], C. Perrin[c], A. Rivaton[b]

[a]*Laboratoire des Matériaux Inorganiques, UMR CNRS 6002, Université Blaise Pascal, 63177 Aubière Cedex, France*
[b]*Laboratoire de Photochimie Moléculaire et Macromoléculaire, UMR CNRS 6505, Université Blaise Pascal, 63177 Aubière Cedex, France*
[c]*Centre de Recherche par Irradiation-CNRS 3A rue de la Ferollerie, 45071 Orléans Cedex 2, France*

Received 1 March 2002; received in revised form 15 July 2002; accepted 16 July 2002

Abstract

Zinc oxide and titanium dioxide coatings were deposited on poly(ether ether ketone) (PEEK) films by r.f. magnetron sputtering from ceramic targets in different argon–oxygen mixtures. PEEK and ceramic/polymer assemblies were irradiated with polychromatic light ($\lambda > 300$ nm). The structure modifications of the surface of irradiated PEEK films were studied by X-ray photoelectron and the rate of photoproducts formation was measured by infra-red and UV–visible spectroscopies. The ZnO coatings were found to protect more efficiently PEEK than TiO_2 coatings. The photoprotective efficiency was shown to depend on the thickness and structural properties of the ceramic coating. The sputtering parameters (total pressure, plasma composition, r.f. power) were optimised in order to limit the photodegradation of the polymer.

Keywords: Poly(ether ether ketone); Photooxidation; Photolysis

1. Introduction

Poly(ether ether ketone) exhibits many interesting characteristics in terms of chemical and mechanical properties. Nevertheless, this polymer suffers a low resistance to sunlight leading to a pronounced photo-yellowing and to a severe loss of physical properties.

A first study has been devoted to the mechanisms of PEEK photodegradation under irradiation at long wavelengths ($\lambda > 300$ nm) in the absence and in the presence of oxygen [1]. It was shown that PEEK photodegradation results from direct absorption of UV–visible radiations by the basic backbone structure of PEEK. The photolytical processes that occur involve the phototransformation of benzophenone moieties and phenylether groups, namely pinacolisation reaction, photo-Claisen type rearrangement and direct chain scissions. Subsequent H-abstraction leads to the formation of numerous molecular fragments that were identified by HPLC after methanolic extraction. Photoproducts resulting from inter- and intra-molecular phenylation reactions and the formation of light absorbing transients (LATs) account for the photodiscolouration of the irradiated films. Under exposure in aerated media the photochemical evolution of PEEK was shown to be far more complex: it involves photolytic reactions that are likely to occur in the absence and also in the presence of oxygen and photooxidative reactions. The oxidation of the photoproducts resulting from direct phototransformations was shown to occur as well as the oxidative attack of the phenyl moieties via ring fragmentation reactions. If the concentration of IR absorbing products was observed to be higher in aerated media, the yellowing was lower than in the absence of oxygen: some of the yellowing species (LATs) were observed to be easily photooxidised.

When photodegradation results from direct absorption of sunlight radiations by the intrinsic chromophoric groups of the macromolecular chains, the incorporation of UV absorbers to the polymer does not provide efficient photostabilisation. Our method to stabilise PEEK films consists of coating the polymer with a thin ceramic layer. The role of the ceramic layer deposited on the polymer surface is to absorb the incident photons, reducing therefore, the rate of formation of the photolysis products. In addition, when a good adhesion is obtained between the coating and the substrate, the surface layer acts as a barrier to oxygen

* Corresponding author. Tel.: +33-4-73-40-71-77; fax: +33-4-73-40-77-00.
E-mail address: luc.gardette@univ-bpclermont.fr (J.L. Gardette).
[1] Permanent address: Institut Supérieur des Sciences Appliquées et de Technologie de Sousse, 4003 Sousse Ibn Khaldoun, Tunisia.

0032-3861/02/$ - see front matter
PII: S0032-3861(02)00499-8

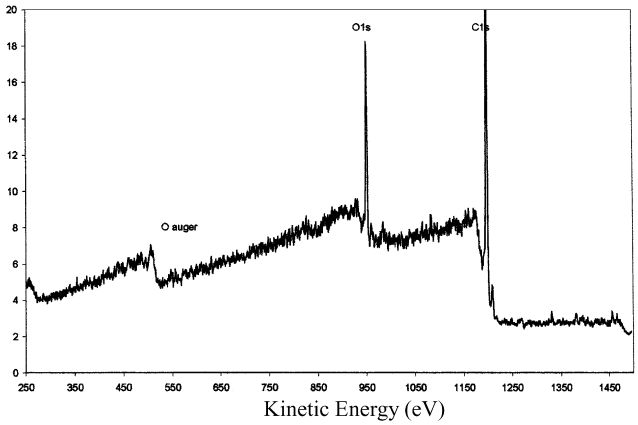

Fig. 1. Complete XPS spectrum of PEEK.

and consequently the rate of formation of the photooxidation products is also anticipated to decrease.

The two ceramics used are zinc oxide (ZnO) and titanium dioxide (TiO_2). These deposits present an intense absorption of the light in the ultraviolet range, and are transparent in the visible range. They have a good chemical stability [2–9]. These coatings were elaborated by r.f. magnetron sputtering, which permits working at low substrate temperature (generally lower than 60 °C). Moreover, the deposits obtained with this technique have a higher density [10,11] and a better adhesion to the substrate than those elaborated by other methods such as vacuum evaporation [4,12,13].

In the first section of this paper, we present a XPS study of irradiated PEEK films to know if the phototransformation at the surface of the samples is similar to the bulk degradation previously determined by IR spectroscopy [1].

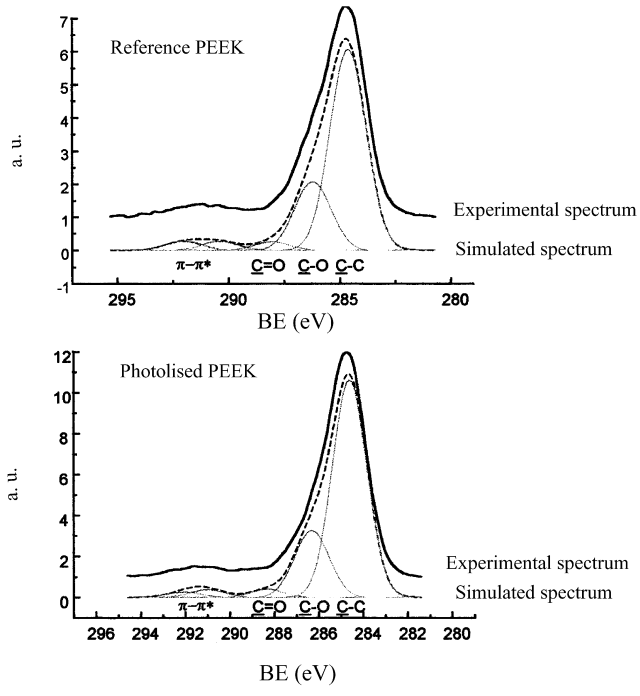

Fig. 2. C_{1s} peak decomposition of reference and photolised PEEK films.

Next, after the characterisation of the phototransformation of PEEK under the ceramic coatings, we focus our investigation on the improvement of the photoprotective effect of the deposits.

2. Experimental

PEEK films (25 μm thick) were commercial grade of Goodfellow. They are amorphous and do not contain antioxidants. They were ultrasonically cleaned in ethanol before irradiation. Irradiations were carried out in a SEPAP 12.24 unit at a temperature of 60 °C. This apparatus permitted irradiation at wavelengths longer than 300 nm. For vacuum photolysis, the samples were introduced in pyrex tubes and sealed under vacuum (10^{-2} Pa).

XPS analyses were achieved under ultra high vacuum in an AEI L200 spectrometer by using Al Kα radiation. The studied area was 5 mm^2. The peak binding energies were referenced to the C_{1s} binding energy of hydrocarbon components fixed at 284.6 eV.

The evolutions of UV and infrared spectra were recorded, respectively, on a Shimadzu UV-2101 PC equipped with an integrating sphere and on a Nicolet Magna-IR 760 FTIR spectrophotometer.

The deposition of ZnO and TiO_2 coatings was carried out in an Alcatel SCM 450 sputtering unit equipped with an r.f. generator operating at 13.56 MHz. Bulk ZnO and TiO_2 targets (purity 99.9%; diameter 100 mm) fixed on cooled magnetron effect cathodes were used as starting materials. The PEEK substrates were situated at a distance of 90 mm from the targets. The sputtering chamber was evacuated below a pressure of 10^{-4} Pa before admitting the sputtering gas which was either pure argon or argon–oxygen mixtures. The plasma composition was controlled by a mass flowmeter. The X-ray diffraction characterisations were carried with a Siemens D501 diffractometer by using Cu $K\alpha_1$ radiation and a Ni filter. The cross-sectional structure of the coatings was observed with a Cambridge Stereoscan 250 scanning electron microscope, the samples were metallized with a thin gold layer to prevent charge built up. For the 180° peeling test, the free polymer surface of the PEEK/ZnO assembly was fixed on a rigid aluminium support using a double sided sticky tape and an EEA copolymer film was thermally bonded on the ZnO coating. The copolymer film was pulling at a 50 mm/min rate.

3. Results and discussion

3.1. XPS analysis

As recalled above, the mechanisms accounting for the photochemical evolution of PEEK irradiated under polychromatic irradiation ($\lambda > 300$ nm) in the absence and in the presence of oxygen have been previously described [1].

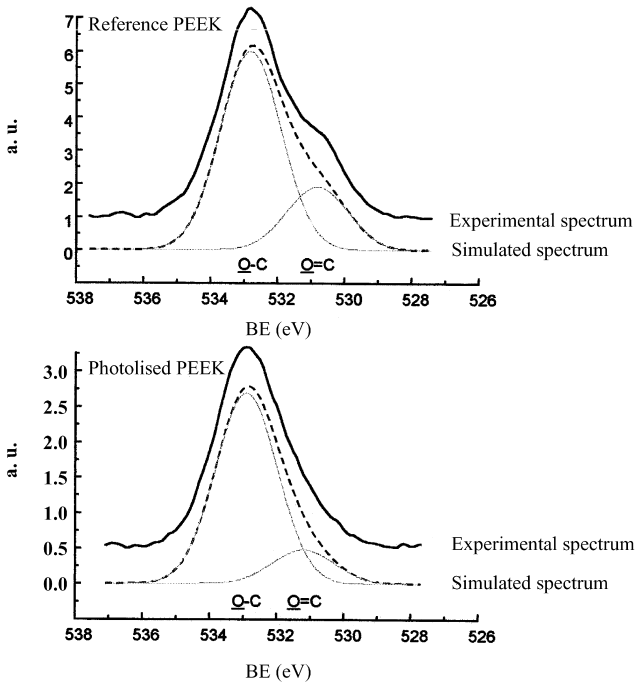

Fig. 3. O_{1s} peak decomposition of reference and photolised PEEK films.

The modifications of the chemical structure of the films (25 μm thick) were monitored by IR and UV–visible transmittance spectroscopies.

In the present study the PEEK surface has been investigated by XPS before and after irradiation. A complete XPS spectrum of a reference (non-irradiated) PEEK is presented in Fig. 1.

Figs. 2 and 3 show the decomposition of C_{1s} and O_{1s} peaks for the reference sample and a PEEK film irradiated under vacuum during 150 h. The contribution of the different components to the total peak are summarised in Tables 1 and 2.

One can note that the photolysis leads to an increase in the number of the C–C bonds at the expense of the C–O bonds. The number of the C=O bonds does not exhibit any significant evolution. These findings indicate the photo-transformation of ether moieties [14,15], confirming previous IR analysis in which direct photodissociative processes were outlined and were shown to be followed by

Table 1
Decomposition of the C_{1s} peak

No.	Attribution	Reference PEEK		Photolised PEEK		Photooxidised PEEK	
		BE (eV)	%	BE (eV)	%	BE (eV)	%
1	C–C	284.6	67	284.6	74	284.6	52
2	C–O	286.2	24	286.3	18	286.4	18
3	C=O	288.0	3	288.3	3	288.5	27
4	$\pi-\pi^*$	290.4	6	291.0	5	291.0	3
5	$\pi-\pi^*$	292.0	6	292.0	5	292.0	3
FWHM (eV)		1.88		1.88		2.03	

Table 2
Decomposition of the O_{1s} peak

No.	Attribution	Reference PEEK		Photolised PEEK		Photooxidised PEEK	
		BE (eV)	%	BE (eV)	%	BE (eV)	%
1	O=C	530.8	28	531.2	19	531.4	58
2	O–C	532.8	72	532.9	81	532.8	42
FWHM (eV)		2.04		2.09		2.03	

radicalar recombination and photo-Claisen type rearrangements. The raise of the number of C–C bonds may justify the inter- and intra- molecular phenylation reactions [1].

The energy shift in C=O from 288 to 288.3 eV results from the formation of carbonyl groups containing other C=O bonds than the initial benzophenone one. This upshot is in good agreement with the identification of ester and aldheydic low molecular weight fragments by HPLC (namely 4-hydroxybenzaldehyde, phenylbenzoate, phenylbenzoquinone and 9-fluorenone). The diminution of the contribution of $\pi-\pi^*$ area confirms the loss of aromaticity of irradiated PEEK in favour of isobenzene structures of 'light absorbing transients' (LATs) [1].

As far as the O_{1s} peak is concerned, one can note an increase in O–C contribution at the expense of O=C bonds. These results coincide with the decrease of benzophenone

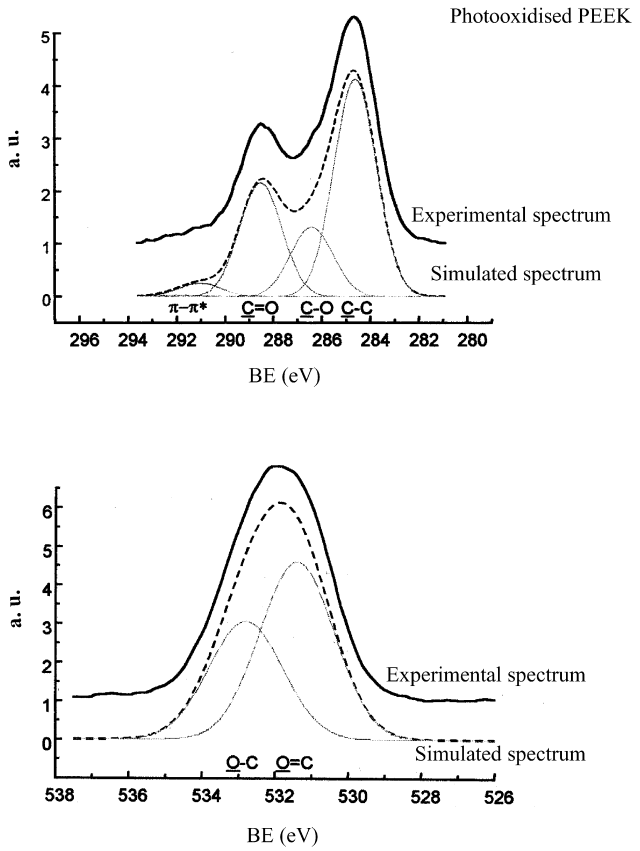

Fig. 4. Decomposition of C_{1s} and O_{1s} peaks of photooxidised PEEK film.

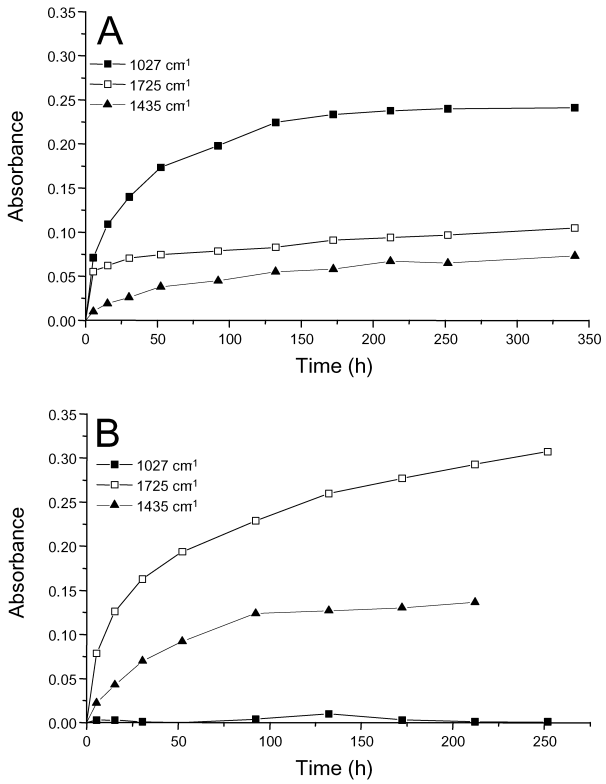

Fig. 5. Increase of absorbance of irradiated PEEK films: (A) photolysis; (B) photooxidation.

moieties and the formation of alcohol groups. In addition the energy shift of O=C component indicates the benzophenone transformation.

When the films are irradiated in the presence of oxygen for 100 h (Fig. 4), one can note a broadening of the different C_{1s} components and an increase in the C=O contribution after irradiation (Table 1). Moreover, the C=O/C–O ratio increases obviously from 0.13 (for the reference PEEK) to 1.5 (for irradiated PEEK).

The energy shift of both C=O and C–O bonds after irradiation accounts for the presence of acid or ester functions. The decrease in the surface aromaticity ($\pi-\pi^*$ transition) corresponds to the opening of aromatic cycles. These findings may explain the formation of aliphatic structures in photooxidised samples.

A high increase in the O_{1s} peak area is noticed, becoming three times more important after polymer photooxidation. The excess oxygen appears mainly in the O=C form. This goes well with the results obtained for the C_{1s} peak decomposition and indicates that the oxidation of the carbonated chains takes place after the opening of the aromatic cycles.

3.2. Measurement of the rate of photoproducts formation

The rate of polymer phototransformation can be characterised by determining the concentration of the stable photoproducts that accumulate in the polymer during irradiation. The concentration is proportional to the increase of absorbance observed on UV–visible and IR spectra.

The photo-yellowing of PEEK throughout exposure can be evaluated by measuring the increase of absorbance at 420 nm. PEEK photooxidation and photolysis was observed to lead also to an increase of absorbance in the hydroxyl, carbonyl and C–O regions of the IR spectra. We noticed the presence of intense bands at 1027 cm^{-1} for photolised samples and at 1435 cm^{-1} when the samples were irradiated in the presence of oxygen [1]. These two absorption bands were not attributed to well-defined structures.

Fig. 5 shows the variation of absorbance at 1725, 1435, and 1027 cm^{-1} versus the irradiation time in the absence and in the presence of oxygen. It can be seen that the rate of phototransformation can be measured by the increase of absorbance as well at 1725 as at 1435 cm^{-1} when the polymer is irradiated in air, at 1725 or at 1027 cm^{-1} when the polymer is irradiated in the absence of oxygen.

Measurements at 1435 and 1027 cm^{-1} have two advantages:

1. Once PEEK is coated with a thin ceramic layer, interference fringes can take place in IR and UV spectra. It is not always possible to eliminate them even by tarnishing the rear surface of the film and by working at the Brewster angle with polarised light. So it can be difficult to characterise accurately the progress of the phototransformation reaction by measuring the absorbance at 1725 cm^{-1} or at 420 nm. On the contrary, the 1500–1000 cm^{-1} region of the infrared spectra is scarcely affected by the interference fringes.
2. The disappearance of the band at 1027 cm^{-1} was observed when PEEK, first irradiated in vacuum, was then irradiated in the presence of oxygen. The band at 1027 cm^{-1} may then be attributed to direct phototransformation products that are unstable in oxygenated media. One can therefore, consider that the analysis of the band at 1027 cm^{-1} during the photooxidation of the PEEK/coating assemblies can account for the PEEK photoprotection mode: absorption of photons and/or decrease in oxygen permeability by the coating.

3.3. Structural properties of ZnO and TiO_2 layers

We have firstly studied the structure and the microstructure of the titania and zinc oxide coatings before the evaluation of their barrier properties against UV radiations.

X-ray diffraction patterns have shown that titanium oxide films deposited on PEEK are amorphous whatever the sputtering parameters are. Similar results were obtained by using electron beam evaporation [16] and ion assisted deposition [17] as elaboration methods. Anatase and rutile phases were observed in our deposits only on heated quartz substrates [18]. The zinc oxide films exhibit a crystallised phase, the würtzite, with a high orientation growth along (002) planes. The *c*-axis orientation was also noted in other

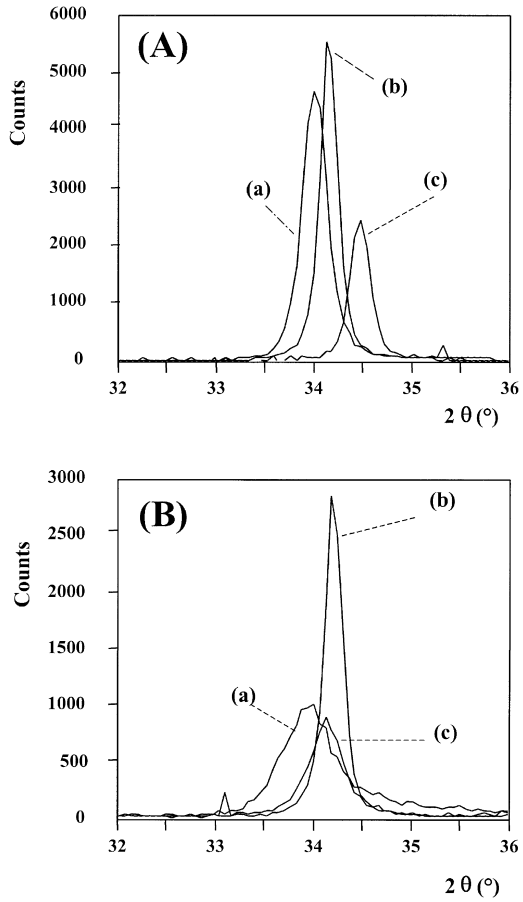

Fig. 6. X-ray diffractograms of ZnO films deposited at (A) different oxygen partial pressures: (a) 0 Pa; (b) 0.01 Pa; (c) 0.05 Pa and at (B) different plasma pressures: (a) 0.2 Pa; (b) 1 Pa; (c) 5 Pa.

researches [19,20]. Some diffractograms are presented in Fig. 6. For the sake of a deeper insight into the film structure, extra slow X-ray diffraction spectra were recorded for diffraction angles between 32 and 36°, the step width and the integration time were 0.004° and 1 s, respectively. The crystallite size representing the longitudinal coherence length in the direction perpendicular to the substrate was deduced from the (002) peak width by using Sherrer formula. The grain size increases all along the coating thickness (Table 3). This evolution can be caused by the thermodynamic coalescence of the crystallites during the film growth [21]. Our findings are in good agreement with Mitra's results [22]. It was found also that the grain size varied from 8 nm for the coating elaborated at a total pressure of 0.2 Pa to 37 nm when the pressure reaches 1.5 Pa. The crystallinity and the grain size are also maximum when a few amount of oxygen is introduced in

Table 3
Variation of the grain size with the ZnO coating thickness

Thickness (nm)	200	400	600	800	1000
Grain size (nm)	25	30	31	34	36

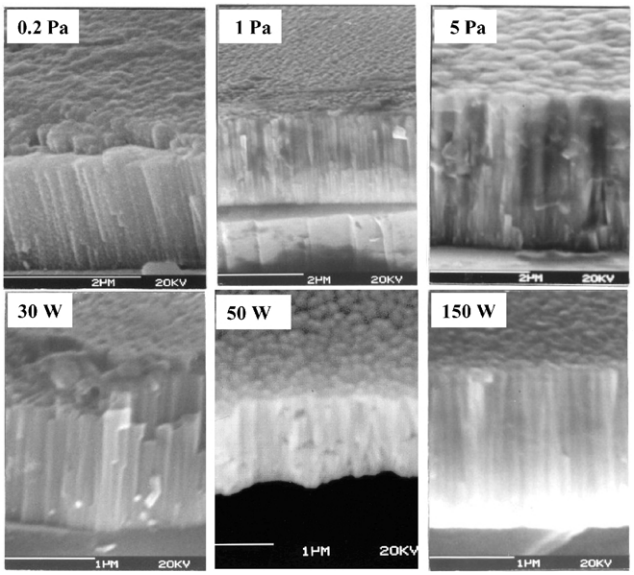

Fig. 7. Scanning electron micrographs of ZnO films deposited at different total pressures (r.f. power: 100 W) and different r.f. powers (total pressure: 1 Pa). The oxygen partial pressure was 0.01 Pa.

the plasma composition and when the applied r.f. power to the target do not exceed 50 W [23].

The scanning electron micrographs of some ZnO films deposited at various conditions are shown in Fig. 7. It was observed that the films develop a columnar microstructure more or less pronounced and normal to the substrate surface. This microstructure originates from the low adatom mobility of the sputtered particles on the substrate surface [24]. It can be seen that the films deposited at low r.f. power present a 'toothed structure' on the top layer, the compactness of the films increases with the r.f. power. However, the films deposited at very high r.f. powers (more than 100 W) were found to exhibit very compressive stresses, mainly intrinsic which can facilitate the disbonding of the coating from the polymer [25]. A compromise is then suitable. We have noted also that the films deposited at intermediate pressures (almost 1.5 Pa) present a regular microstructure with very slightly tapered columns. The variation of the

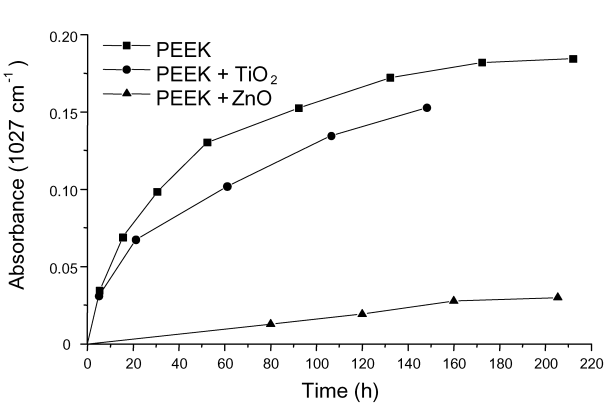

Fig. 8. Variation of absorbance at 1027 cm^{-1} of reference and ceramic coated PEEK films versus the irradiation time in vacuum.

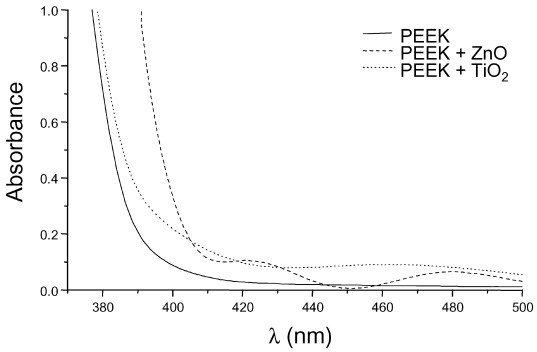

Fig. 9. UV–visible spectra of reference and ceramic coated PEEK films before irradiation.

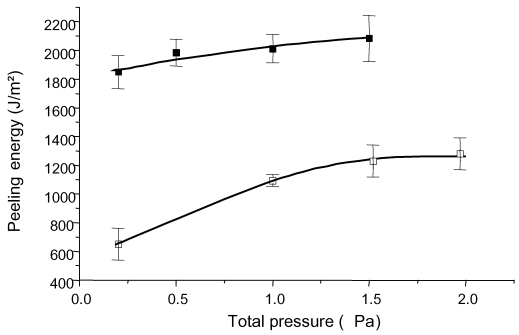

Fig. 10. Evolution of the peeling energy of ceramic coatings on PEEK versus the total pressure: (■) ZnO and (□) TiO_2.

oxygen partial pressure do not influence significantly the evolution of the microstructure of zinc oxide films.

Concerning the titanium oxide films, the coatings deposited at high r.f. powers and low total pressures were found to be compact [26].

3.4. Photoprotective efficiency of ZnO and TiO_2 layers on PEEK

Fig. 8 shows the variation of absorbance at 1027 cm^{-1} versus irradiation time in vacuum for PEEK films uncoated and coated on both faces by ZnO or TiO_2 layer (2 × 800 nm). When the polymer is coated with a ZnO layer, the rate of phototransformation sharply decreases (by a factor of 6.5 after 200 h of irradiation). The diminution is less notable in the case of TiO_2 coatings.

The UV–visible spectra and the absorption percentage which are reported in Fig. 9 and Table 4, respectively, allow to compare the absorption properties of ZnO and TiO_2 coatings in the UV–visible region. The absorption of incident UV-light is higher for ZnO than TiO_2. This result permits explaining the kinetic data reported in Fig. 8: a non-negligible part of the incident photons which are the most damageable for the photostability of PEEK are not absorbed by the TiO_2 deposit and reach the surface of the polymer, causing therefore, its photodegradation.

Moreover, the adhesion strength (determined by the standard peeling test) of zinc oxide films on PEEK was found to be much more important than the titania one (Fig. 10). This can allow the zinc oxide coatings to protect more efficiently the polymer. It is obvious to note also that the peeling energy increases with the total pressure. It reaches its maximum value (2200 J/m^2) when the r.f. power is around 75 W, i.e. when the coatings are compact and when the stress level is low [25].

In addition it is worthy to note that we have shown in the previous work [23] by combining XPS, peeling and fragmentation measurements that the adhesion of zinc oxide films on PEEK is narrowly correlated to the kinetic energy of sputtered particles which intervene directly on the polymer surface, the PEEK surface treatments by cold plasmas before deposition have a negligible influence on the adherence in comparison with the atomic bombardment occurring during the coating growth.

Fig. 11 shows the variation of absorbance at 1435 cm^{-1} versus the irradiation time in the presence of oxygen for PEEK films uncoated and coated on both faces by ZnO or TiO_2 layer (2 × 800 nm).

As observed in the absence of oxygen, ZnO coating protects efficiently the polymer and TiO_2 deposit slows down the rate of photoproducts formation in the first time (almost during 150 h). However, in the second stage, TiO_2 deposit increases the rate of photodegradation. This increase may be attributed to the photocatalytic properties of TiO_2 [27,28]. The excitation of the thin TiO_2 layers generates the formation of activated species (mainly $OH^{\cdot}$, $HO_2^{\cdot}$ radicals) which are susceptible to initiate photooxidation reactions from the surface of the coated polymer.

Table 4
Absorption of ceramic coatings at different wavelengths

λ (nm)	TiO_2 absorption (%)	ZnO absorption (%)
370	32.9	96.1
380	29.0	96.1
390	29.2	86.4
400	25.8	43.3
410	21.1	14.1
420	21.5	16.1

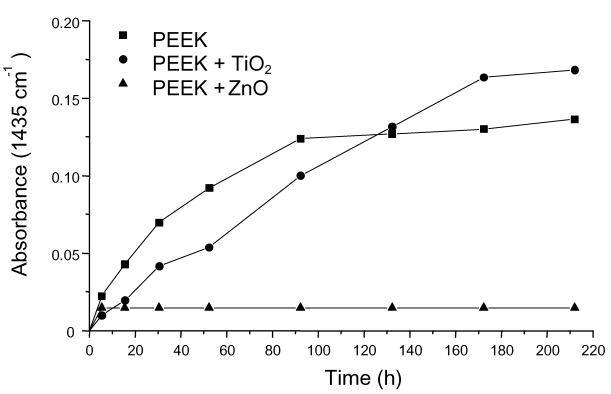

Fig. 11. Variation of absorbance at 1435 cm^{-1} of reference and ceramic coated PEEK films versus the irradiation time in presence of oxygen.

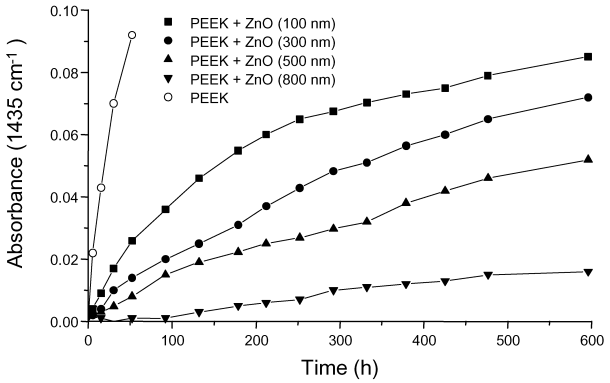

Fig. 12. Variation of absorbance at 1435 cm^{-1} of PEEK films coated with ZnO deposits of different thickness.

3.5. PEEK photoprotection by ZnO layer

The decrease in the rate of photodegradation of the coated polymer could depend not only on the nature of the ceramic layer but also on its properties (structure, microstructure, composition, optical properties), and its adhesion strength on the polymer. In this scope, we have varied the sputtering parameters of a ZnO layer (which exhibits the most interesting photoprotective properties) in order to optimise the PEEK photoprotection.

3.5.1. Influence of the coating thickness

Several ZnO coatings with different thickness were elaborated on PEEK films. Fig. 12 shows the variation of absorbance at 1435 cm^{-1} of the different polymer/ceramic assemblies versus the irradiation time. One can note that the rate of photooxidation decreases when the thickness of the coating increases. As shown in this figure, the photoprotective effect is very efficient when the thickness is 800 nm (which corresponds to a grain size of 34 nm).

In order to outline the inhibition factor due to ZnO photoprotection, we measured the increase in absorbance at 1435 cm^{-1} of the coated PEEK after 600 h of irradiation. Then we determined the duration of irradiation t necessary so that the increase in absorbance at 1435 cm^{-1} of a non-coated PEEK reaches the same value. The inhibition factor f_i is given by the following relationship: $f_i = 600/t$.

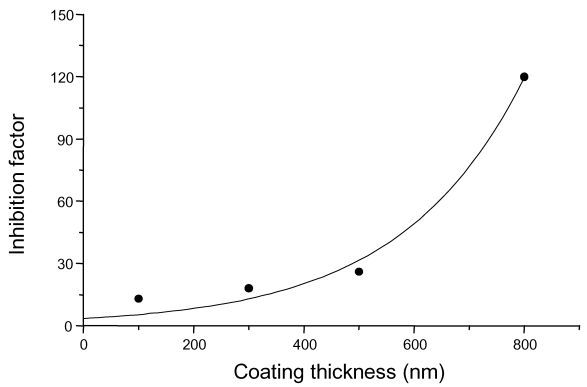

Fig. 13. Variation of the inhibition factor versus the thickness of the ZnO coating.

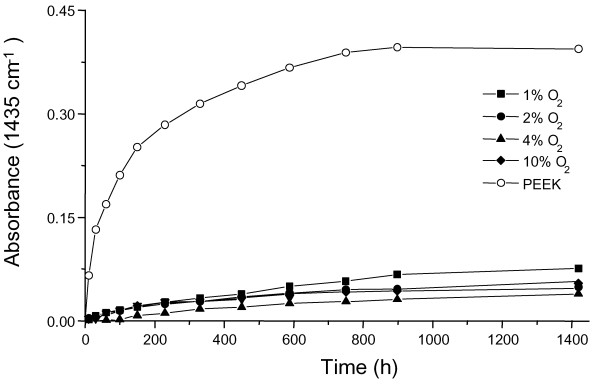

Fig. 14. Variation of absorbance at 1435 cm^{-1} versus the irradiation time for PEEK films coated with ZnO deposits (500 nm thick, 100 W power, 1 Pa pressure, various plasma compositions).

The evolution of f_i with the coating thickness is presented in Fig. 13. To reduce the photodegradation of PEEK, it is worthy to diminish the absorption of incident light by the polymeric substrate. When the thickness increases, the coating grain size increases and the intensity of absorbed radiations by PEEK decreases (screen effect). We note that f_i follows an exponential variation as the classical light absorption law (Beer–Lambert). This curve is in good agreement with our previous findings [1]: the first stage of PEEK photodegradation in oxygenated media involves direct absorption of incident light by the chromophoric groups of the polymer.

3.5.2. Influence of the deposition conditions

We have deposited ZnO coatings of 500 nm thick with various sputtering parameters: the plasma composition, the r.f. power and the total pressure. It can be seen that the oxygen percentage in the plasma has only a slight influence on the photooxidation rate (Fig. 14). The lowest rate was obtained at a power of 75 W using a sputtering gas containing 4% of oxygen (Fig. 15). The total pressure has a stronger effect on the photoprotective behaviour of the

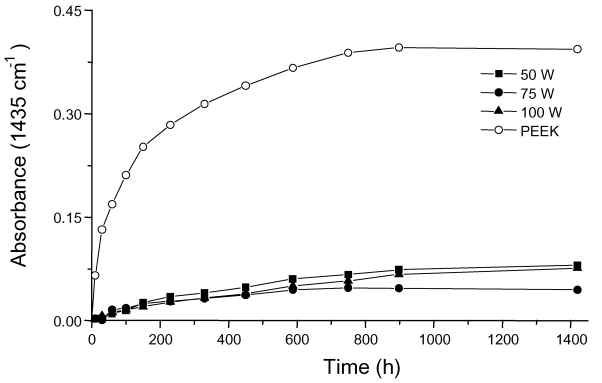

Fig. 15. Variation of absorbance at 1435 cm^{-1} versus the irradiation time for PEEK films coated with ZnO deposits (500 nm thick, $Ar–O_2$ (1%) plasma, 1 Pa pressure, various powers).

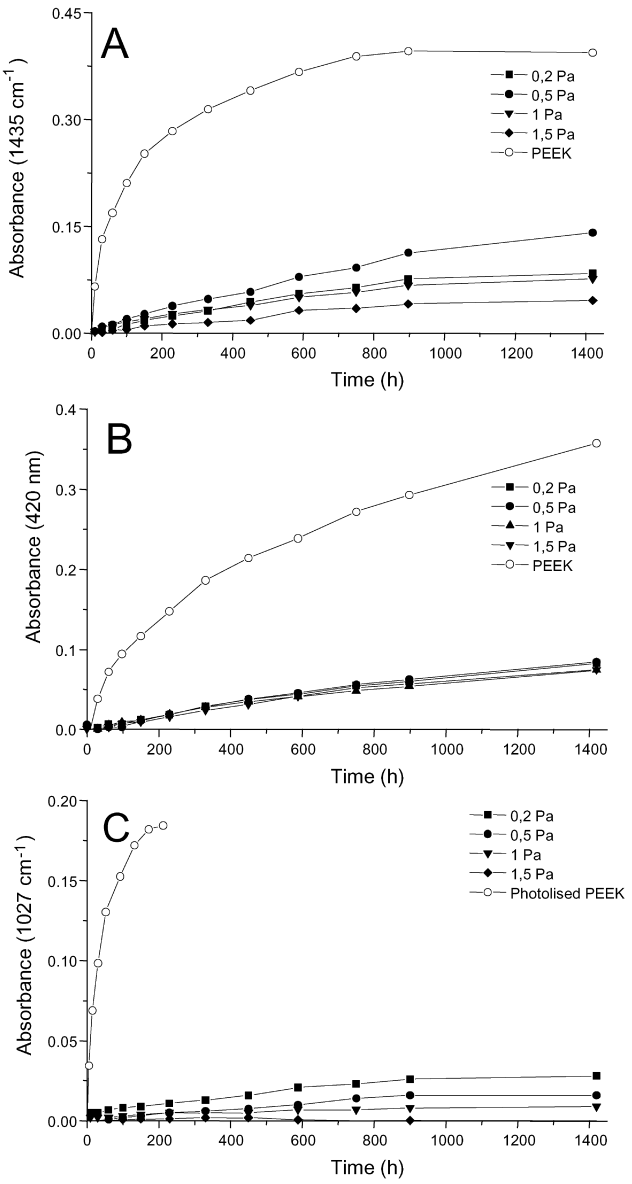

Fig. 16. Variation of absorbance at: (A) 1435 cm^{-1}, (B) 420 nm and (C) 1027 cm^{-1} versus the irradiation time for PEEK films coated with ZnO deposits (500 nm thick, 100 W power, $Ar-O_2$ (1%) plasma, various pressures).

coating (Fig. 16). The rate of formation of photooxidation products decreases when the coatings are elaborated at high total pressures equivalent to 1.5 Pa.

The initial absorbance (before irradiation) of the coating in the UV–visible range was calculated and found to be more important in the case of deposits made at high pressures. In such conditions, the coating is more adherent on PEEK; it presents a regular structure, has a high grain size and protects more efficiently the polymer against incident radiation.

To examine the photolytic process contribution (without intervention of oxygen) to the photooxidation of PEEK/ZnO assemblies, the variation of absorbance at 1027 cm^{-1} was measured (Fig. 16). The increase of absorbance was found to be more important at low sputtering pressures. This result means that the lower the pressure, the lower the coating oxygen permeability. The coatings elaborated at low pressure are almost amorphous. In the case of high pressure, the kinetic energy of the sputtered particles is sufficient for producing surface diffusion and the crystallinity (würtzite form of ZnO) is improved. The amorphous coatings are the most impermeable to oxygen.

The photocolouration of the polymer measured by the increase in absorbance at 420 nm is globally the same whatever the sputtering conditions are. This may be explained according to the photolysis/photooxidation duality taking place during PEEK irradiation.

4. Conclusion

The XPS analysis of the chemical modifications that occur at the surface of PEEK films irradiated with polychromatic wavelengths show that the phototransformation of the surface is analogous to the one of the core of the sample as previously determined by IR spectroscopy [1]. Coating PEEK by ZnO and TiO_2 thin layers increases its photostability. This effect can be attributed to the screen effect played by the layer of ceramic. ZnO presents a higher photoprotective efficiency than TiO_2, which can be attributed to a higher absorption ability in the UV–visible range. The coating photoprotective effect increases all along with the coating thickness, i.e. when the absorption of incident radiation by the polymer decreases. To a smaller extent, the deposition properties were also found to influence the photooxidation rate, namely the crystallinity which is strictly correlated to the total pressure. The best PEEK photostability was obtained by sputtering at a 75 W power with an $Ar-O_2$ (4%) plasma at a pressure of 1.5 Pa. In such conditions, the zinc oxide film is also strongly bonded to the polymer.

References

[1] Giancaterina S, Rossi A, Rivaton A, Gardette JL. Polym Degrad Stab 2000;68:133.
[2] Yoshikawa H, Adachi S. Jpn J Appl Phys 1997;36:6237.
[3] Dumont E, Dugnoille B, Bienfait S. Thin Solid Films 1999;353:93.
[4] Swamy HG, Reddy PJ. Semicond Sci Technol 1990;5:980.
[5] Schropp REI, Madan A. J Appl Phys 1989;66:2027.
[6] Blom FR, Van de Pol FCM, Bauhuis G, Pompa TJA. Thin Solid Films 1991;204:365.
[7] Proscia J, Gordon RG. Thin Solid Films 1992;214:175.
[8] Reddy PS. Solid State Commun 1991;77:899.
[9] Ben Amor S, Baud G, Jacquet M, Pichon N. Surf Coat Technol 1998; 102:63.
[10] Meng LJ, Andritschky M, Dos Santos MP. Appl Surf Sci 1993;65/66: 235.
[11] Whicaksana D, Kobayashi A, Kinbara A. J Vac Sci Technol, A 1992; 10(4):1479.
[12] Kim JS, Marzouk HA, Reucroft PJ. Thin Solid Films 1992;217:133.

[13] Watanabe H. Jpn J Appl Phys 1970;9:418.
[14] Kharasch MS, Stampa G, Nudenberg W. Science 1952;116:309.
[15] Hageman HJ, Louwerse HL, Mijs WJ. Tetrahedron 1971;26:2045.
[16] Gofuku E, Toyoda Y, Vehara Y, Kohara M, Nunoshita M. Appl Surf Sci 1991;48(49):343.
[17] Krishana MG, Narasimha Rao K, Mohan S. J Appl Phys 1983;73:434.
[18] Ben Amor S, Guedri L, Baud G, Jacquet M, Ghedira M. Mater Chem Phys 2002; in press.
[19] Natsume Y, Sakata H. Thin Solid Films 2000;372:30.
[20] Lu YM, Hwang WS, Liu WY, Yang JS. Mater Chem Phys 2001;72: 269.
[21] Lodder JC, Wiellinga T, Worst J. Thin Solid Films 1983;101:61.
[22] Mitra A, Thareja RK, Ganesan V, Gupta A, Sahoo PK, Kulkarni VN. Appl Surf Sci 2001;174:232.
[23] Giancaterina S, Ben Amor S, Bachari EM, Baud G, Jacquet M, Perrin C. Surf Coat Technol 2001;138:84.
[24] Thornton JA. J Vac Technol 1976;11:666.
[25] Giancaterina S. Thesis. Clermont Ferrand University, France; 2000.
[26] Ben Amor S, Baud G, Besse JP, Jacquet M. Mater Sci Engng 1997; B47:110.
[27] Ginhac JM. Thesis. Clermont Ferrand University, France; 1980.
[28] Bourasseau S, Martin JR, Juillet F, Teichner SJ. J Chim-Phys 1974;7–8:71.